Journal of Mining and Geology Vol. 57(2) 2021. pp. 315 - 322 0022-2763

Geoelectrical Investigation of Soil Corrosivity and Aquifer Protective Capacity in Angware and Its Environs, Jos-Plateau, Northcentral Nigeria

Bulus, J.A.[1] and Odewumi, S.C.[2]
[1]Department of Geology, University of Jos, Jos, Nigeria
[2]Department of Science Laboratory Technology, University of Jos, Jos, Nigeria
Corresponding E-mail: sholaodewumi@yahoo.com

Abstract
Geoelectrical resistivity method was adopted in the study of soil corrosivity and aquifer protective capacity (APC) in Angware and its environs, Jos-Plateau. This present study focuses on delineating zones that are very prone to groundwater contamination from surface contaminants and subsurface soils that are corrosive to utility pipes. Seventy-four (74) vertical electrical sounding (VES) stations were occupied in Angware and Its Environs with current spacing (AB/2) ranging from 1 to 125 m using Schlumberger array. ABEM SAS 300C terrameter was used to generate the data. The interpretations of the VES data were supported by WinResist, Excel and surfer software. The geoelectric sections indicate four (4) layers which include: topsoil, clayey layer, fractured basement and fresh basement while two (2) major aquiferous units identified were weathered basement and fractured basement with thickness of 11.30 to 41.07 m. Topsoil resistivity values were adopted in classification of soil corrosivity and four zones of soil corrosivity were recognized in the area namely: very strongly corrosive zone (< 10 Ωm), moderate corrosivity zone (10 - 60 Ωm), slightly corrosivity zone (60 - 180 Ωm) and practically noncorrosive zone (> 180 Ωm). The value of longitudinal conductance of the overburden units varies from 0.008523 to 1.829263 mhos and four (4) aquifer protective capacity zones were delineated based on the longitudinal conductance values namely: poor (< 0.1 mhos), weak (0.1–0.19 mhos), moderate (0.2–0.69 mhos) and good (0.7–4.49 mhos). The poor and weak aquifer protective capacity zones could be vulnerable to surface contamination, while the good and moderate aquifer protective capacity zones have higher protection against surface contaminated fluids and are apparently safe.

Keywords: *Overburden, Geoelectric, corrosivity, protective and aquifer.*

Introduction

Groundwater encompasses water that exists in the subsurface and is contained in geologic formation called aquifers. Aquifers are geological formations that are porous and permeable which retained and released water (Wightman *et al.,* 2003; Todd and Mays, 2005). The soils and rocks resistivities depend largely on properties of rocks which include permeability, soil porosity, ionic value of the pore fluids, and clay mineralization and these differ with time and space (Oseji, 2010). Geophysical techniques have been applied for groundwater contamination studies (Kelly, 1976; Benson *et al.,* 1997; Arristodemou and Thomas-Betts, 2000; Adepelumi *et al.,* 2001; Naudet *et al.,* 2004). Geoelectrical methods were developed to demarcate locations prone to contamination (Braga *et al.,* 2006; Atakpo and Ayolabi, 2009; Mogaji *et al.,* 2007; Abiola *et al.,* 2009).

Angware area occurs in Jos East Local Government Area of Plateau State on Longitudes 9.09095^0 to 9.13888^0 E and Latitudes 9.97981^0 to10.01461^0 N (Fig. 1). Angware area is located in the Guinea Savannah region with scattered trees and is typified by wet and dry seasons. The Geological setting of the study area is characterized by basement rocks namely: migmatite, fine to medium-grained biotite and biotite muscovite granite and Neil's Valley granite porphyry (Figure 2). Due to the increasing population of Angware area, industrial and domestic wastes were being generated which may contaminate the groundwater. This present study focuses on delineating zones that are very prone to groundwater contamination from surface contaminants and subsurface soils that are either corrosive or non-corrosive to utility pipes.

Materials and Methods

Schlumberger electrode array with half-current electrode separation (AB/2) ranging from 1 to 125 m was adopted in the field measurements and geoelectrical survey involving 1-D VES readings. Seventy-four (74) VES stations were occupied in Angware area and ABEM SAS 300C terrameter was used to generate the data. The coordinates of the VES station was taken with the Garmin handheld Global Positioning System (GPS) device for longitude and latitude readings while the data sheet was used for recording field data.

Resistivity data were inverted using WinResist software program and was design to avoid the curve-matching method. Filed data were uploaded into the program window and the software generates a curve of apparent resistivity plotted against electrode separation (AB/2). An inversion was then run until a perfect match was obtained and necessary monitoring of the process must be ensured for precision. The total longitudinal

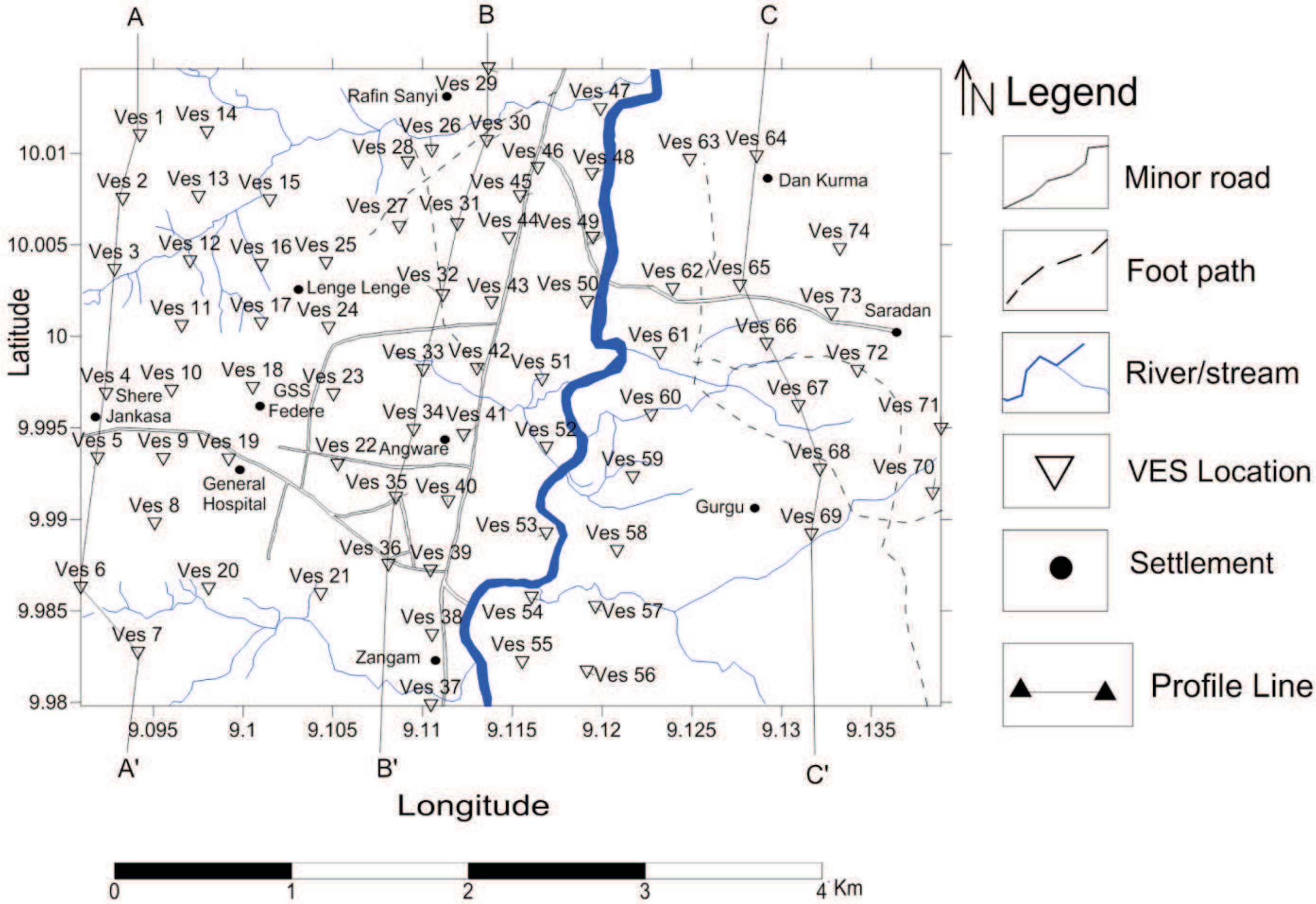

Fig. 1: Topographical map of Angware and environs with Profile lines and VES locations

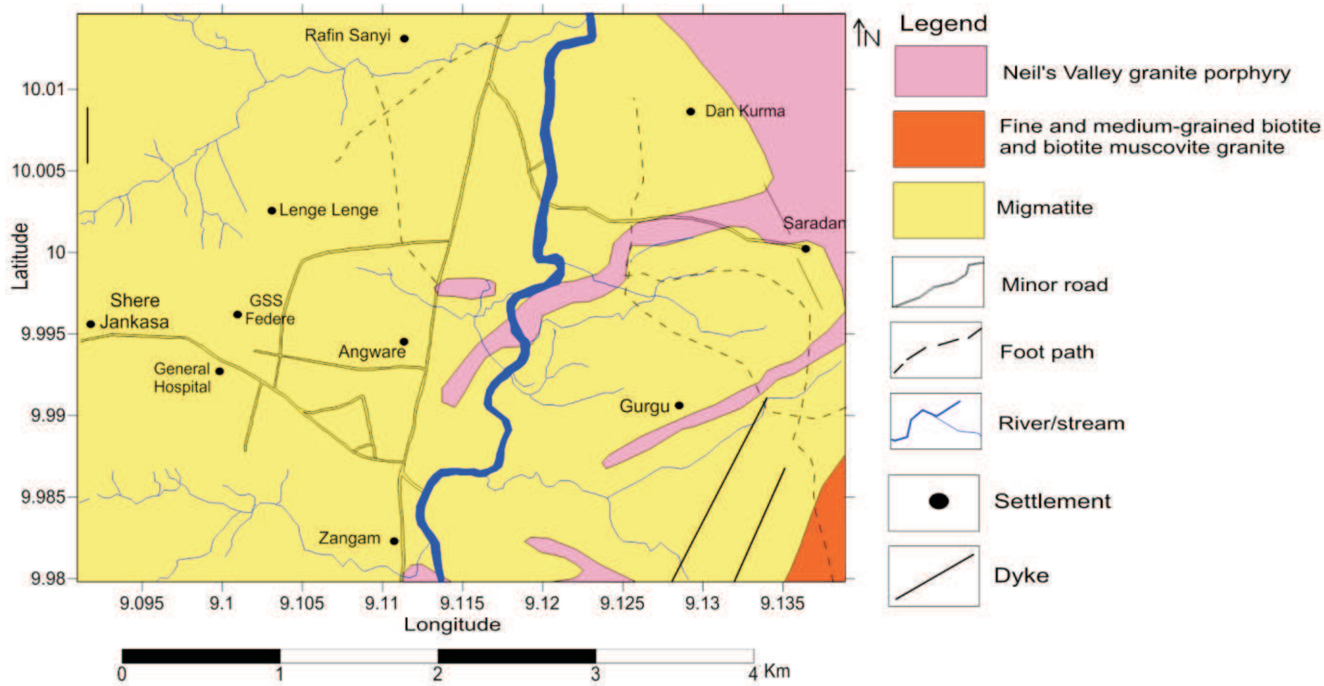

Fig. 2: Geological map of Angware and environs.

conductance (S) of Angware and environs was estimated from equation after Zohdy *et al.*, (1974)

$$S = \Sigma (hi/\rho i) = h1/\rho 1 + h2/\rho 2 + \ldots\ldots + hn/\rho n$$

Where **S** is the total longitudinal conductance,
Σ is summation sign,
hi is thickness of the nth layer and ***ρ*i** is resistivity of the nth layer.

Results

The values of layer resistivity and layer thickness obtained from the seventy-four (74) VES stations are presented in Table 1. The curve types, longitudinal conductance values and aquifer thickness are also presented in Table 1. The sounding curves found within the study area have 3-layer model (A, H and Q); 4-layer model (AA, HA, HK, KH, QH and QQ) and 5-layer model (HAA) of geoelectrical layers (Table 1). The geoelectric section ranges from 3 to 5 layers with the 3-layer as the dominant type (Table 2). Figure 3 shows the representative VES curves in Angware and its environs which include: Q-curve, QH-curve, HA-curve and AA-curve. Figure 4 shows the frequency of curve type distribution in Angware and its environs.

Discussion

Aquifer Units within the Area

The weathered and fractured zone thickness of Angware and its environs (Figure 5) indicates that the highest thickness of weathered layer unit of about 41.07m was identified at VES 50 and the thickness of the weathered layer unit with the lowest thickness of about 11.3m occurs at VES 71 and VES 73. Thus, the thickness of weathered and fractured layers of Angware and its environs is relatively high for groundwater accumulation. The two (2) aquifer units within the area include the weathered layer and fractured basement. The weathered aquifer (porous and not permeable) is incompetent, fragile and easily collapse when drill hole is left without support inside it while the fractured basement aquifer is competent and permeable. The two aquifer types are connected together with the weathered aquifer overlying the competent fractured basement aquifer.

Evaluation of Soil Corrosivity

The thickness of the topsoil layer varies from 0.5 to 17.4 m and the resistivity varies from 9.2 to 3257.4Ωm. The topsoil resistivity values obtained from the study area (Table 1) was adopted in the interpretations and evaluation of the corrosivity as shown in Figure 6. Topsoil resistivity values were used in the classification of soil corrosivity based on the classification of Baeckmann and Schenwenk (1975); Agunloye (1984) and Oladapo *et al*. (2004). The low topsoil resistivity values of < 10 Ωm indicates very strongly corrosive and the resistivity values ranging from 10 to 60 Ωm denotes moderate corrosivity zones while the topsoil resistivity values ranging from 60 to 180 Ωm represents slightly corrosivity zones and areas with resistivity values of > 180 Ωm indicates practically noncorrosive (Figure 5).

Evaluation of Aquifer Protective Capacity

The values of longitudinal conductance were adopted to classify overburden units into good, moderate, weak and poor aquifer protective capacity zones based on the classification of Henriet (1976) and Oladapo *et al*. (2004). The longitudinal conductance of 0.7 to 4.9 mhos indicates good aquifer protective capacity and longitudinal conductance of 0.2 to 0.69 shows moderate aquifer protective capacity while longitudinal conductance of 0.1 to 0.19 mhos indicates weak aquifer protective capacity and longitudinal conductance of <0.1 mhos shows poor aquifer protective capacity. The highest longitudinal conductance value of 1.829263 mhos was identified at VES 21 and lowest longitudinal conductance value of 0.008523 mhos was identified at VES 16 (Table 1).

The good and moderate aquifer protective capacity zones coincide with zones of considerable overburden thicknesses with high clay column and low resistivity value while the weak and poor zones coincide with zones of shallow or thin overburden thickness and high electrical resistivity value. Yellow and powder blue colours areas are covered by poor and weak Aquifer protective capacity zones and they may be vulnerable to surface contamination sources such as leakage from underground petroleum storage tanks, infiltration of leachates from decomposing of open refuse dumps and diffuse pollution from agricultural activities within the study area (Figure 7).

The good (pink colour) and moderate (cyan colour) aquifer protective capacity zones of the study area have higher protection against surface contaminated fluids so that in the face of contamination such zones are apparently safe (Figure 7). High total longitudinal

Table 1: Layers resistivity, thickness, curve types, longitudinal conductance and aquifer thickness.

	Resistivity (Ohm-m)					Thickness (m)						
VES Station	ρ_1	ρ_2	ρ_3	ρ_4	ρ_5	h_1	h_2	h_3	h_4	Curve Type	Longitudinal Conductance (mhos)	Aquifer Thickness (m)
1	490.6	207.7	250			5.2	30			Q	0.155038	36.47
2	381.2	113.7	82.2			3.1	19.1			Q	0.176118	38.57
3	340.2	78.4	109.8			1.9	33.6			H	0.434156	39.77
4	424.3	169.8	130			9.0	20			Q	0.138997	32.67
5	306.8	212.0	192.2			2.6	14.7			Q	0.077814	39.07
6	720.9	94.6	424.9			10.8	15.7			H	0.180943	30.87
7	572.4	312.2	276.5			2.0	7.1			Q	0.026236	39.67
8	488.7	204.6	87.0			2.6	44.8			Q	0.224284	39.07
9	292.1	65.7	374.3			1.3	34			H	0.521954	40.37
10	748.2	211.4	23.2	574.1		1.1	8.1	19.4		QH	0.875993	40.57
11	453.1	239.7	95.1	536.5		1.4	9.7	26.0		QH	0.316954	40.27
12	343.6	245.1	104.2			1.3	8.4			Q	0.038055	40.37
13	702.2	128.0	50.2			0.8	6.9			Q	0.055046	40.87
14	933.9	239.8	162.7			3.6	20.2			Q	0.088092	38.07
15	656.9	335.1	254.7			3.2	7.1			Q	0.026059	38.47
16	2218.1	456.0	1113.8	183.9		1.1	1.9	4.3		HK	0.008523	34.27
17	372.2	122.2	698.0			2.9	26.3			H	0.16463	38.77
18	762.2	763.9	81.6	195.0		4.9	3.2	7.6		KH	0.103755	36.77
19	665.9	166.1	37.4	393.4		8.5	4.8	21.6		QH	0.619203	33.17
20	899.6	485.4	164.4			1.3	9.0			Q	0.019986	40.37
21	86.6	31.1	11.2			2.2	56.1			Q	1.829263	39.47
22	3257.4	237.5	65.8	244.6		1.5	5.5	42.0		QH	0.661916	40.17
23	935.7	200.8	41.5	716.1		1.7	7.5	13.7		QH	0.369288	39.97
24	2793.8	1328.0	229.5	158.8		0.6	6.6	2.7		QQ	0.016949	37.07
25	352.7	278.6	38.9	553.3		3.6	3.4	13.9		QH	0.379737	38.07
26	331.2	109.5	1501.4			1.7	28.3			H	0.26358	39.97
27	104.1	44.0	596.1			1.2	30.9			H	0.7138	40.47
28	434.5	184.8	44.2			2.8	23.6			Q	0.13415	38.87
29	444.6	198.0	28.0	887.3		2.5	3.2	12.0		QH	0.450356	39.17
30	1015.1	262.2	232.0	293.1		2.0	2.5	12.7		QH	0.066246	39
31	296.6	70.3	704.5			1.7	10.2			H	0.13415	39.97
32	115.4	48.1	147.0	2614.5		0.6	13.5	8.5		HA	0.103755	22.6
33	795.1	47.6	354.7			0.6	24.2			H	0.509158	41.07
34	1284.0	292.9	33.0	1080.4		1.9	8.9	16.9		QH	0.543987	27.7
35	948.7	500.4	127.8	147.8		3.7	2.1	3.6		QH	0.036266	37.97
36	138.4	319.2	1441.9			11.5	11.6			A	0.119433	23.1
37	47.5	91.0	288.6	615.3		11.4	7.5	19.7		AA	0.390678	38.27
38	564.9	32.2	137.3	1335.8		0.5	5.0	18.0		HA	0.287264	23.5
39	185.3	87.1	265.3	830.9		1.9	3.0	15.7		HA	0.103875	39.77
40	229.8	70.3	2701.2			2.5	18.9			H	0.279727	21.4
41	808.4	131.1	57.2	2659.2		1.6	3.5	14.3		QH	0.278676	19.4
42	280.5	71.0	570.8			1.6	13.9			H	0.201479	40.07
43	18.0	79.1	928.7			0.8	31.4			A	0.44141	40.87
44	264.4	116.0	1317.2			0.8	25.2			H	0.220267	26
45	912.0	112.3	19.8	992.7		0.8	1.0	13.0		QH	0.666348	40.87
46	783.5	218.2	24.3	1443.6		0.8	4.8	9.6		QH	0.418081	15.2
47	52.7	36.8	19.8			1.8	20.3			Q	0.585786	39.87
48	26.6	65.2	16.9	128.3		1.8	6.4	14.9		KH	1.047485	39.87
49	9.2	33.3	260.5			5.3	16.9			A	1.083594	36.37
50	199.4	29.5	59.3	611.3		0.6	3.1	25.9		HA	0.544856	41.07
51	169.3	100.6	89.9	673.6		2.6	13.1	23.4		QH	0.405865	39.07
52	129.2	39.2	580.6	85.5		1.8	4.5	25.9		HK	0.173337	39.87
53	106.3	170.4	35.9	254.3		2.9	4.4	17.0		KH	0.52664	38.77
54	267.7	50.3	355.9			3.2	30.0			H	0.608375	38.47
55	101.3	90.1	27.1	320.7		2.7	3.8	15.6		QH	0.644475	38.97
56	181.3	88.7	60.0	636.9		1.4	11.0	18.8		QH	0.445069	40.27
57	23.1	1802.0	2100.0			17.4	20			A	0.764346	17.4
58	460.8	32.6	36.0	1056.5		1.0	8.2	8.9		HA	0.500926	18.1
59	289.1	105.7	116.6			3.6	1.2			H	0.023805	38.07
60	244.2	36.3	540.4			1.0	20.9			H	0.579853	40.67
61	187.5	915.5	257.2	220.2		3.6	8.1	19.6		KH	0.104253	38.07
62	251.1	65.3	1535.9			2.8	25.3			H	0.398594	28.1
63	445.5	138.8	87.2			2.3	14.9			Q	0.112511	39.37
64	761.6	16.9	2164.7			4.7	9.6			H	0.574219	14.3
65	157.0	63.0	110.9	378.0		5.8	8.0	14.2		HA	0.29197	35.87
66	438.4	37.8	67.4	185.0	2818.5	0.6	2.4	13.6	8.2	HAA	0.310965	24.8
67	35.5	13.4	138.4	3009.4		1.0	7.1	6.4		HA	0.604263	14.6
68	23.5	113.6	360.7	1747.7		4.5	4.6	10.3		AA	0.260538	19.4
69	389.6	88.1	235.2	148.5		2.3	3.6	25.8		HK	0.15646	39.37
70	554.5	235.2	408.5			1.5	14.2			H	0.063079	40.17
71	199.8	42.4	834.3	3333.8		1.2	3.7	6.4		HA	0.100941	11.3
72	14.5	44.3	2694.0			1.0	18.6			A	0.48883	19.6
73	332.3	41.3	3761.7			1.2	10.1			H	0.248163	11.3
74	614.3	253.2	125.9	314.7		1.3	6.3	46.1		QH	0.393161	40.37

VES = vertical electrical sounding, $\boldsymbol{\rho_1}$= first-layer resistivity, $\boldsymbol{\rho_2}$= second-layer resistivity, $\boldsymbol{\rho_3}$= third-layer resistivity, $\boldsymbol{\rho_4}$= fourth-layer resistivity, $\boldsymbol{\rho_5}$= fifth-layer resistivity, $\mathbf{h_1}$= first-layer thickness, $\mathbf{h_2}$= second-layer thickness, $\mathbf{h_3}$= third-layer thickness, $\mathbf{h_4}$= fourth-layer thickness, m = meters.

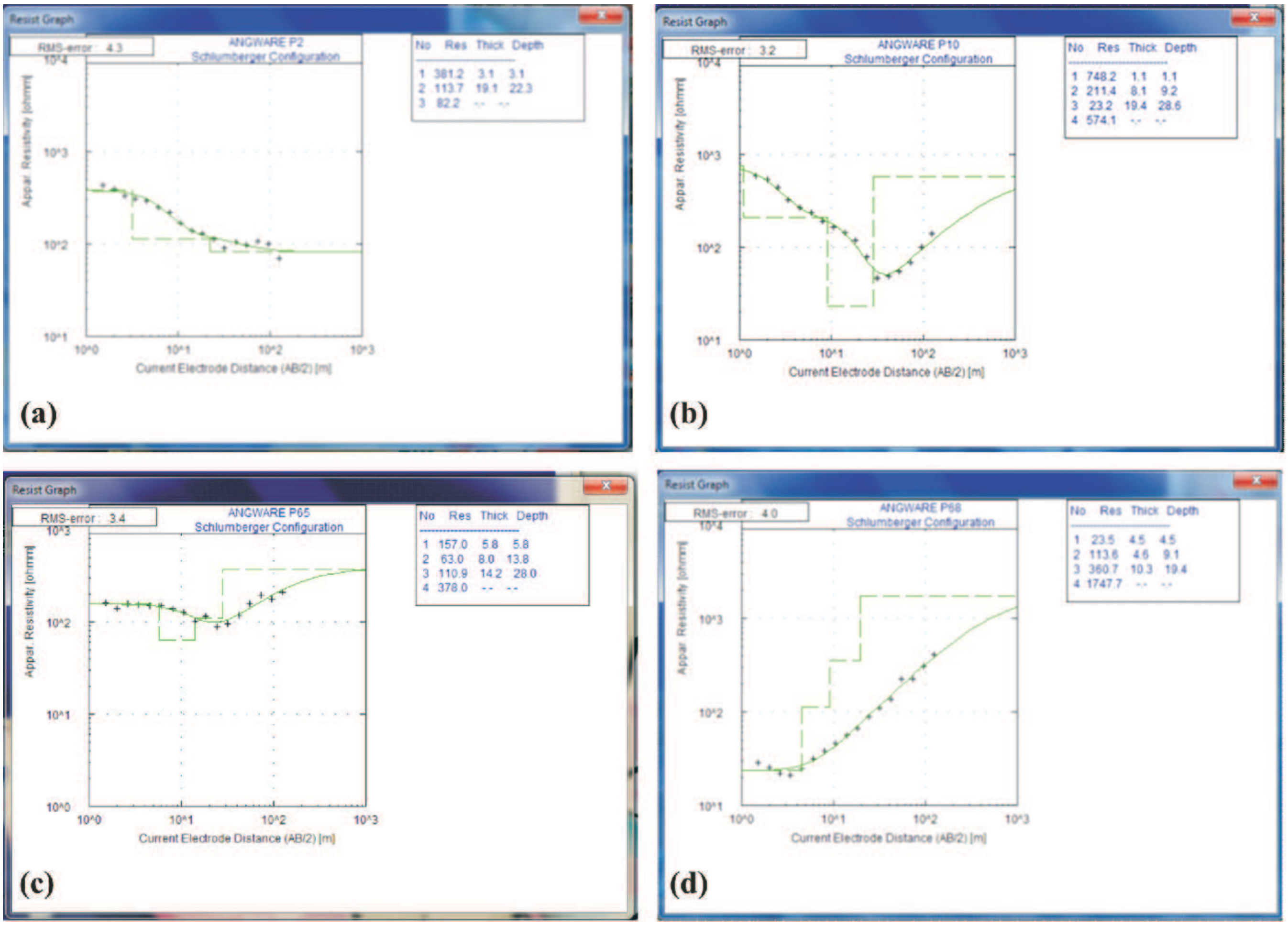

Fig. 3: Representative VES curve in Angware and its environs (a) Q curve, (b) QH curve, (c) HA curve and (d) AA curve.

Table 2: Qualitative analysis of curve types

S/No	Curve Types	Frequency	Percentage (%)	Layer's resistivity Relationship	Number of geoelectric layers
1	A	5	6.76	$\rho 1 < \rho 2 < \rho 3$	3
2	Q	15	20.27	$\rho 1 > \rho 2 > \rho 3$	3
3	H	18	24.32	$\rho 1 > \rho 2 < \rho 3$	3
4	AA	2	2.7	$\rho 1 < \rho 2 < \rho 3 < \rho 4$	4
5	HA	8	10.81	$\rho 1 > \rho 2 < \rho 3 < \rho 4$	4
6	HK	3	4.06	$\rho 1 > \rho 2 < \rho 3 > \rho 4$	4
7	KH	4	5.41	$\rho 1 < \rho 2 > \rho 3 < \rho 4$	4
8	QH	17	22.97	$\rho 1 > \rho 2 > \rho 3 < \rho 4$	4
9	QQ	1	1.35	$\rho 1 > \rho 2 > \rho 3 > \rho 4$	4
10	HAA	1	1.35	$\rho 1 > \rho 2 < \rho 3 < \rho 4 < \rho 5$	5
Total		74	100		

Note: ρ– resistivity

conductance (S) values are indicative of deeper basement while low value of total longitudinal conductance (S) represent shallow basement and an increase in the total longitudinal conductance (S) value may correspond to a typical increase in the clay content and consequently a decrease in the transmissivity of the aquifer (Oteri, 1981; Khali, 2009).

In this study, low values of the total longitudinal conductance (<0 – 0.19 mhos) correspond with deeper basement with comparable thick aquifer units at VES 1, VES 2, VES 4, VES 5, VES 12, VES 13, VES 14, VES

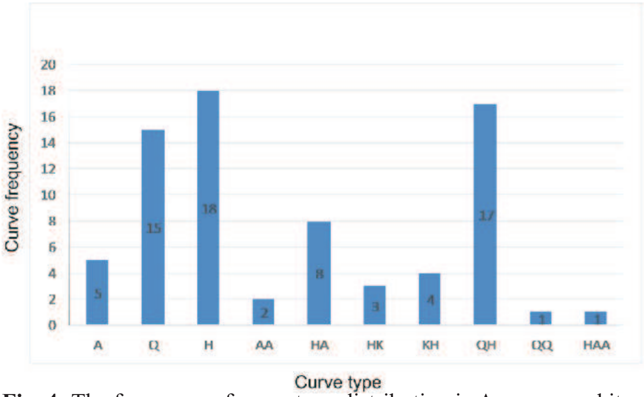

Fig. 4: The frequency of curve type distribution in Angware and its environs

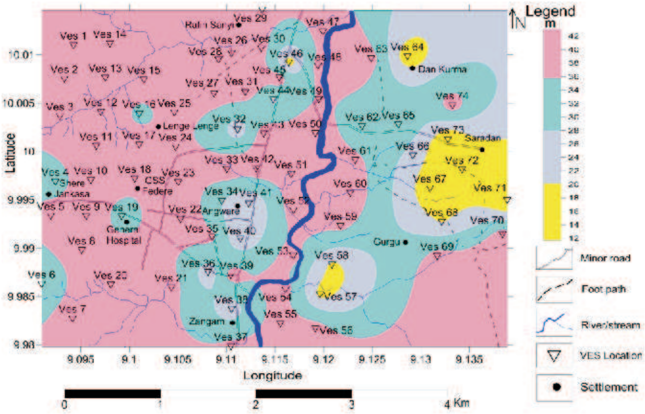

Fig. 5: Aquifer thickness map of Angware and environs

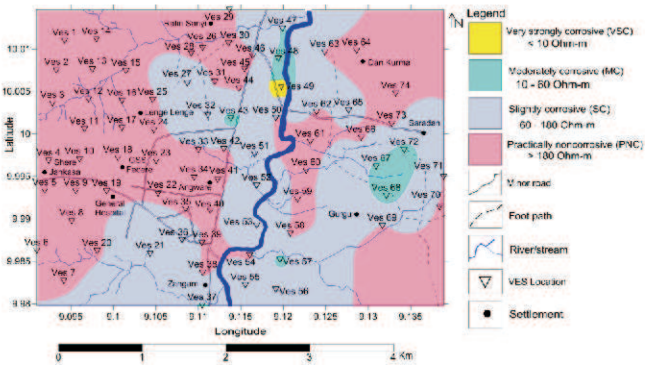

Fig. 6: Soil corrosivity map of Angware and its environs with VES location

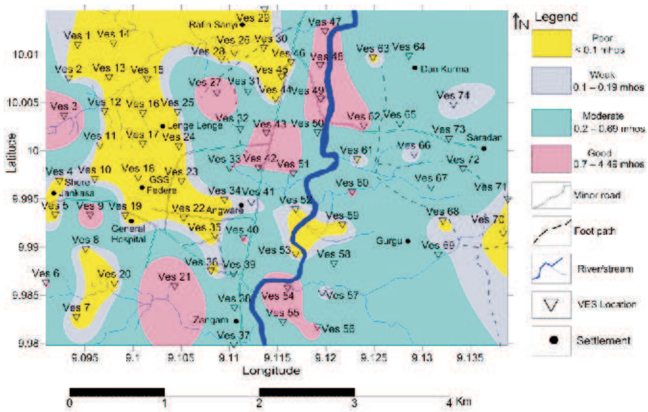

Fig. 7: Longitudinal Conductance map of Angware and environs

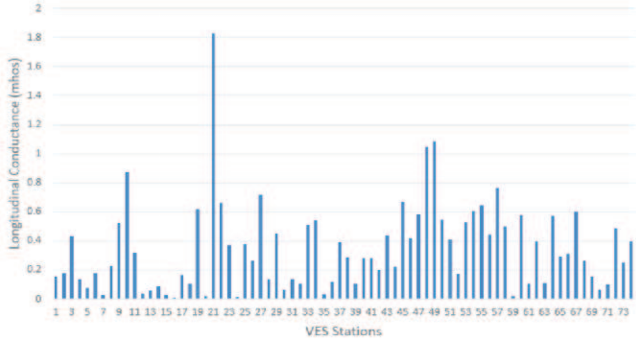

Fig. 8: A graph of Longitudinal Conductance map of Angware and environs

15, VES 16, VES 17, VES 18, VES 20, VES 24, VES 28, VES 30, VES 35, VES 59, VES 63, and VES 70. This inconsistency could only come from the differences in geologic terrain and is in contrast with report of Oteri (1981) in sedimentary area. The study also revealed high values of total longitudinal conductance (0.20 - 1.829263 mhos) as shown in Table 1 with thick aquifer devoid of clay layer above it at VES 8, VES 10, VES 11, VES 19, VES 21, VES 22, VES 23, VES 25, VES 29, VES 45, VES 53 and VES 74 (Figure 8). Hence, the absent of clay content over the aquifer will increase its transmissivity and render it susceptible to surface fluid contaminants (Adeniji *et al.*, 2014).

Geo-Electric Sections

The 2-D geoelectric sections (Figs. 9a - c) were all plotted in the north-south directions along A-A, B-B and C-C Profile lines (Figure 1). Three (3) distinctive geoelectric layers were identified in A-A profile section as shown in Figure 9a. The topsoil has resistivities of 340.2 to 720.9 ohm-m and thickness values of 1.90 to 10.80 m. The second layer consists of clay/fractured basement with resistivities value of 78.4 to 94.6 Ohm-m and thickness of 15.7 to 33.6 m. The very thick clay layer underlying the topsoil was observed at VES 3 and VES 6 while the fractured basement across the section was located at VES 1, VES 2, VES 4, VES 5 and VES 7 with their resistivities value of 113.7 to 312.2 ohm-m and thickness of 7.1 to 30 m. The third layer consists of fractured basement with resistivities of 82.2 to 424.9 ohm-m and an infinite depth. This A-A profile has very thick aquifer (Fig. 9a) and is good for groundwater production with the exclusion of VES 3 which has a thick clay layer. Oteri (1981) and Khali (2009) reported that an increase in the clay content will decrease the transmissivity of the aquifer and render it unproductive for groundwater production.

Four (4) distinct geoelectric layers were identified in B-B profile section as shown in Figure 9b. The topsoil resistivities value of 115.4 to 1284 Ohm-m and thickness of 0.6 to 11.5 m. The second layer consists of clay with resistivities of 48.1 to 70.3 Ohm-m and thickness of 10.2 to 24.2 m. The third layer consists of fractured/fresh basement, the fractured basement is superimposed by clay layer at VES 31, VES 32 and VES 33 across the section with resistivities of 28 to 704.5 Ohm-m and thickness of 3.6 to 16.9 m while the fresh basement is located only at VES 36 having resistivity value of 1441.9 Ohm-m with an infinite thickness. The fourth layer consists of fractured/fresh basement, VES 29, VES 30 and VES 35 constitute the fractured basement having resistivities of 147.8 to 887.3 Ohm-m with an infinite thickness, while the fresh basement underlies VES 32 and VES 34 with an unlimited thickness. The aquifer thickness at VES 32 and VES 36 are not thick enough to support groundwater production.

Four (4) distinct geologic layers were identified along the C-C Profile as shown in Figure 9c. The topsoil resistivities range from 35.5 to 761.6 ohm-m with thickness of about 0.6 to 5.8 m. The second layer consists of clay unit underlying the topsoil at VES 64, VES 65, VES 66, VES 67 and VES 69 with resistivities of 13.4 to 88.1 Ohm-m and thickness of 2.4 to 9.6 m. The third layer comprises of fractured/fresh basement with the fractured basement having resistivity of 67.4 to 360 Ohm-m and thickness of 6.4 to 25.8 m while the fresh basement was identified at VES 64 with resistivity of 2164.7 Ohm-m having an infinite thickness. The fourth layer also consists of fractured/fresh basement with the fresh basement underlying VES 66, VES 67 and VES 68 representing the impermeable layer having resistivities of 1747.7 to 3009.4 ohm-m with an inestimable thickness. Only VES 65 and VES 69 were recommended for locating borehole owing to their thick aquifer and clay layer overlying this location in order to prevent contamination from surface fluid infiltration.

Conclusion

The sounding curves show three to five model layers namely: three (3) layer model (A, H and Q); four (4) layer model (AA, HA, HK, KH, QH and QQ); and five (5) layer model (HAA) geoelectric layers with the 3-layer model as the dominating type.

The geoelectric sections along the profiles revealed three to four subsurface layers namely: the topsoil, clayey layer, fractured basement and the fresh basement. The two major aquiferous units were the weathered layer and fractured basement.

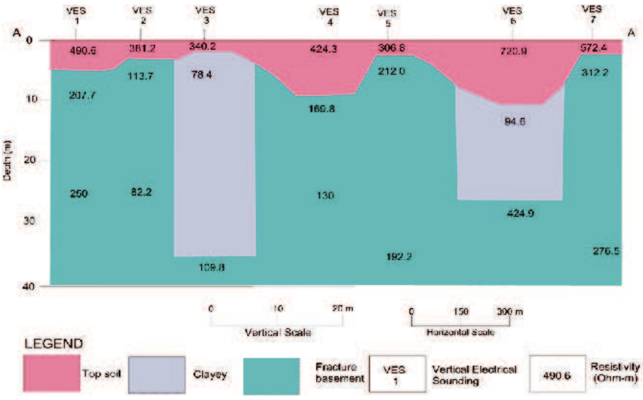

Fig. 9a: Geoelectric Section along Profile A-A'

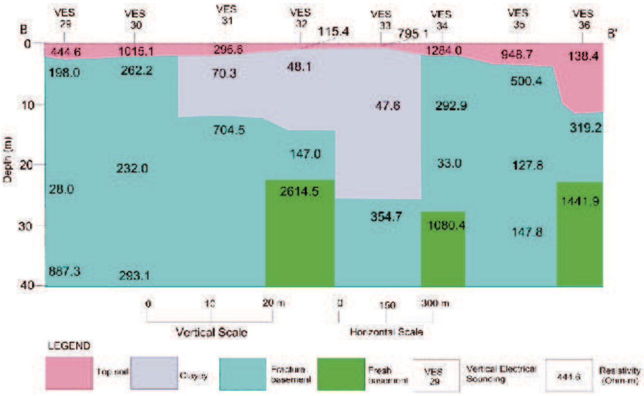

Fig. 9a: Geoelectric Section along Profile A-A'

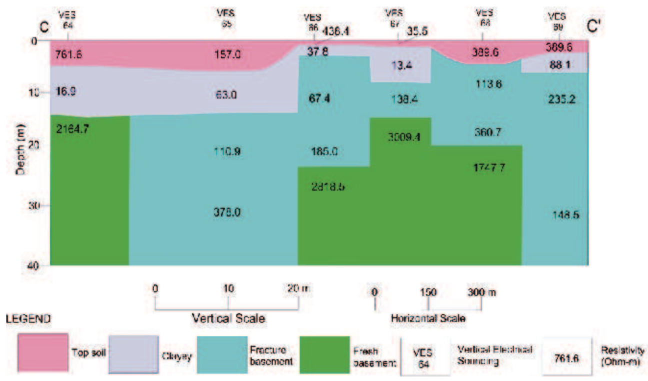

Fig. 9a: Geoelectric Section along Profile A-A'

The topsoil resistivity values were adopted soil corrosivity classification and four zones of soil corrosivity were recognized in the area namely: very strongly corrosive zone (< 10 Ωm), moderate corrosivity zone (10 - 60 Ωm), slightly corrosivity zones (60 - 180 Ωm) and practically noncorrosive (> 180 Ωm). Four (4) aquifer protective capacity zones were identified in Angware and its environs based on the longitudinal conductance values namely: good, moderate, weak and poor. The good and moderate aquifer protective capacity zones have higher protection against surface contaminated fluids and are apparently safe.

References

Abiola, O., Enikanselu, P. A. and Oladapo, M. I. (2009). Groundwater potential and aquifer protective capacity of overburden units in Ado-Ekiti, southwestern Nigeria. International Journal of Physical Science, 4(3), pp. 120 - 132.

Adeniji, A.E., Omonona, O.V., Obiora, D.N. and Chukudebelu, J.U. (2014). Evaluation of soil corrosivity and aquifer protective capacity using geoelectrical investigation in Bwari basement complex area, Abuja. Journal of Earth System Science, 123(3), pp. 491 - 502.

Adepelumi, A.A., Ako, B.D. and Ajayi, T.R. (2001). Groundwater contamination in the basement complex area of Ile-Ife southwestern Nigeria: A case study using the electrical resistivity geophysical method. Hydrogeology Journal, 9, pp. 611 - 622.

Agunloye, O. (1984). Soil aggressivity along steel pipeline route at Ajaokuta southwestern Nigeria. Journal of Mining Geology, 21, pp. 97 - 101.

Arristodemou, E. and Thomas-Betts, A. (2000). DC resistivity and induced polarization investigations at a waste disposal site and its environments. Journal of Applied Geophysics, 44, pp. 275 - 302.

Atakpo, E.A. and Ayolabi, E.A. (2009). Elevation of aquifer vulnerability and protective Capacity in some oil producing communities of western Niger delta. Environmental, 29, pp. 310 - 317.

Baeckmann, W.V. and Schwenk, W. (1975). Handbook of cathodic protection: The theory and practice of electrochemical corrosion protection technique. Surrey Protucullin Press

Benson, A.K., Payne, K.L. and Stubben, M.A. (1997). Mapping groundwater contamination using DC resistivity and VLF geophysical methods: a case study. Geophysics, 62, pp. 80 - 86.

Braga, A.O., Filho, W.M. and Dourado, J.C. (2006). Resistivity (DC) method applied to aquifer protection studies. Revista Brasileira Geofisica, 24(4), pp. 513 - 581.

Henriet, J.P. (1976). Direct application of the Dar Zarrouk parameters in groundwater surveys. Geophysical Prospect, 24, pp. 344 - 353.

Khalil, M.H. (2009). Hydrogeophysical assessment of Wadi El-Sheikh aquifer, Saint Katherine, South Sinai, Egypt. Journal of Environmental and Engineering Geophysics, 14(2), pp. 77-86

Kelly, W.E. (1976). Geoelectric sounding for delineating groundwater contamination. Groundwater, 4, pp. 6-10.

Mogaji, K.A., Adiat, K.A.N. and Oladapo, M.I. (2007). Geoelectric investigation of the Dape Phase111 Housing Estate FCT Abuja northcentral Nigeria. Journal of Earth Science, 1(2), pp. 76 - 84.

Naudet, V., Revil, A., Rizzo, E., Bottero, J.Y. and Begassat, P. (2004). Groundwater redox conditions and conductivity in a contaminant plume from geoelectrical investigations; Hydrology. Journal of Earth Science, 8(1), pp. 8 - 22.

Oladapo, M.I., Mohammed, M.Z., Adeoye, O.O. and Adetola, O.O. (2004). Geoelectric investigation of the Ondo State Housing Corporation Estate, Ijapo, Akure southwestern Nigeria. Journal of Mining Geology, 40 (1), pp. 41 - 48.

Oseji, J.O. (2010). Geoelectrical investigation of groundwater resources and aquifer characteristics in Utagba-Ogbe Kingdom Nvokwa Land Delta State Nigeria. Journal of Environmental Chemistry and Ecotoxicology, 2(3), pp. 38 - 46.

Oteri, A.U. (1981). Geoelectric investigation of saline contamination of chalk aquifer by mine drainage water at Tilmanstone, England. Geoexploration, 19, pp. 179 - 192.

Todd, D.K. and Mays, L.W. (2005). Groundwater Hydrology; John Wiley and Sons, New York.

Wightman, W. E., Jalinoos, F., Sirles, P. and Hanna, K. (2003). Application of geophysical methods to highway related problems; Federal Highway Administration, Central Federal Lands Highway Division, Lakewood, Publication. FHWA-IF-04-021.

Zohdy, A.A.R., Eaton, G.P. and Mabey, D.R. (1974). Application of surface geophysics to groundwater investigations; United State Geophysical Survey, Washington.